

# MULTI-OTR SYSTEM FOR LINEAR COLLIDERS\*

J. Resta-López, A. Faus-Golfe, IFIC (CSIC-UV), Valencia, Spain  
 J. Alabau-Gonzalvo, R. Apsimon, A. Latina, CERN, Geneva, Switzerland

## Abstract

We study the feasibility of using a multi-Optical Transition Radiation (m-OTR) system for fast transverse emittance reconstruction and x-y coupling correction in the Ring to Main Linac (RTML) of the future linear colliders: ILC and CLIC. OTR monitors are mature and reliable diagnostic tools that could be very suitable for the setup and tuning of the machine in single-bunch mode. Here we study the requirements for a m-OTR system adapted to the optical conditions and beam parameters of the RTML of both the ILC and CLIC.

## INTRODUCTION

The control and the preservation of low emittance along the transport through the different subsystems of the future linear colliders will be essential to obtain the required luminosity. Diagnostic stations in the different transfer lines are dedicated to emittance measurement and control.

The m-OTR system in the ATF2 extraction line [1] has shown to be very reliable for performing fast emittance measurements and contributing efficiently to the tuning of the beamline. Here we explore the feasibility of using a m-OTR system in transfer lines of the RTML. OTR monitors could be very suitable for the setup and tuning of the machine in single-bunch mode. It can be very useful during startup and commissioning phases of the RTML when operating in low charge mode (single-bunch mode). In this paper we investigate different materials for the OTR target and possible limitations of operation in the context of both the ILC and CLIC RTML.

In principle the OTRs can coexist with laser wire scanners [2]. While the OTRs are intended for relatively low beam power use, the laser wire scanners will be necessary for beam size measurements and emittance reconstruction during the multi-bunch train operation. When operating with high charge and multi-bunch train the OTRs would be in non-measurement mode, i.e. they would be retracted from the beam path.

## M-OTR SYSTEM FOR THE ILC RTML

The ILC RTML has recently been updated and optimised, and a complete description can be found in [3]. The RTML is divided in the following sections, indicated in Fig. 1: Ring To Linac (RTL), Long Transfer Line (LTL), Turnaround (TURN), Spin Rotator (SPIN), first and second stages of the Bunch Compressor (BC1/BC2) and their

respective dump lines. These structures are present in both electron and positron beamlines.

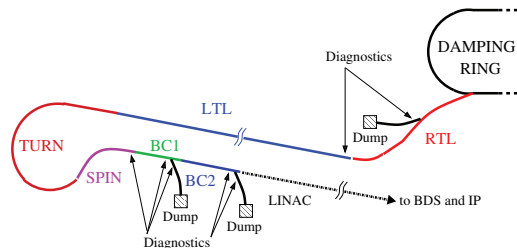


Figure 1: Schematic of the ILC RTML for the electron beam.

The ILC RTML has been designed with 7 diagnostic sections: beginning of LTL, end of SPIN, end of BC1 and BC2, and in each dump line. Here we study the following important cases: assuming m-OTR systems at the beginning and at the end of the RTML. Table 1 shows the beam parameters at the beginning of the LTL (Start RTML) and downstream of the BC2 (End RTML) of the ILC RTML.

Table 1: Beam parameters at the beginning and at the end of the ILC RTML.

Parameter	Start RTML	End RTML
Energy	5 GeV	15 GeV
Number of particles per bunch	$2 \times 10^{10}$	$2 \times 10^{10}$
Bunch length	6 mm	0.3/0.15 mm
Energy spread	0.13%	1.07%
Normalised H. emittance	8 $\mu\text{m}$	8 $\mu\text{m}$
Normalised V. emittance	20 nm	20 nm

Figure 2 shows the optics of LTL and a zoom of the lattice where we tentatively suggest possible positions for OTRs. The LTL lattice mainly consists of FODO cells with  $\mu_{x,y} = \pi/4$  phase advance. The positions that we suggest here would be alright for projected emittance measurement (2D reconstruction). In this case the optimum transverse phase advance between measurement stations is  $\pi/N$ , with  $N$  the number of stations ( $N = 4$  OTRs in our case). For coupling correction skew quadrupoles can be placed in the FODO cells upstream of this system. More general optical conditions also valid for 4D emittance reconstruction can be found in Ref. [4].

Figure 3 shows the diagnostic section at the end of the RTML, where we can locate another m-OTR system. This section is downstream of BC2, in the linac launch.

## OTR Target Damage Study

The passage of one pulse through an OTR target leads to the following peak of instantaneous temperature rise in the material:

\* Work supported by grant FPA2010-21456-C02-01 from Ministerio of Economía y Competitividad, Spain.

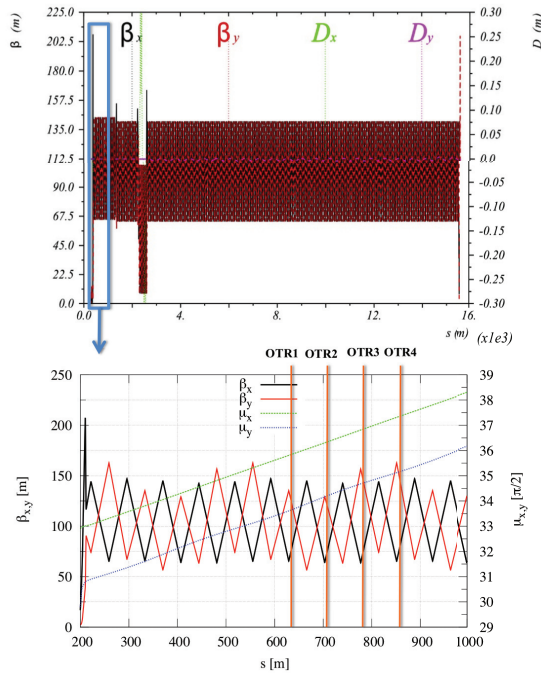


Figure 2: Optics layout of the ILC LTL. Positions of 4 OTRs for a 2D emittance reconstruction section are indicated.

$$\Delta T_{inst} = \frac{1}{\rho C_p} \left( \frac{dE}{dz} \right) \frac{N_b N_e}{2\pi\sigma_x\sigma_y}, \quad (1)$$

where  $\rho$  is the material density,  $C_p$  the specific heat,  $N_e$  the number of particles per bunch, and  $N_b$  the number of bunches per train ( $N_b = 1$  for OTR operation).  $dE/dz$  is the collision stopping power (ionization) calculated using the Bethe-Bloch formula. Here the target is supposed to be thin enough ( $< 1$  radiation length) to neglect radiation stopping power.

The rapid heating of the material caused by the impact of a pulse in the OTR target may contribute to the fracture of the material by thermal stress. The increment of temperature which determines the limit for thermal induced mechanical fracture can be analytically evaluated using the following expression:  $\Delta T_{fr} \cong 2\sigma_{UTS}/(\alpha_T Y)$ , where  $\sigma_{UTS}$  is the ultimate tensile strength,  $\alpha_T$  is the thermal expansion coefficient and  $Y$  the modulus of elasticity. Thermal and mechanical properties for several materials are summarised in Table 2 [5]. In order to avoid damage to the target, we have selected a set of materials with a relatively high melting temperature ( $T_{melt}$ ), a high specific heat ( $C_p$ ) and a high thermal conductivity ( $k$ ). It is necessary to mention that Kapton is a material that does not melt but decomposes at 793 K.

Let us first study the case of an OTR located at the beginning of the LTL, where we can find approximately the following beam sizes:  $\sigma_x \approx 239.14 \mu\text{m}$  ( $\beta_x \approx 70 \text{ m}$ ) and  $\sigma_y \approx 17.49 \mu\text{m}$  ( $\beta_y \approx 150 \text{ m}$ ). The results for the temperature rise of material per pulse ( $\Delta T_{inst}$ ), in comparison with the temperature rise for fracture limit ( $\Delta T_{fr}$ ), are shown in

ISBN 978-3-95450-122-9

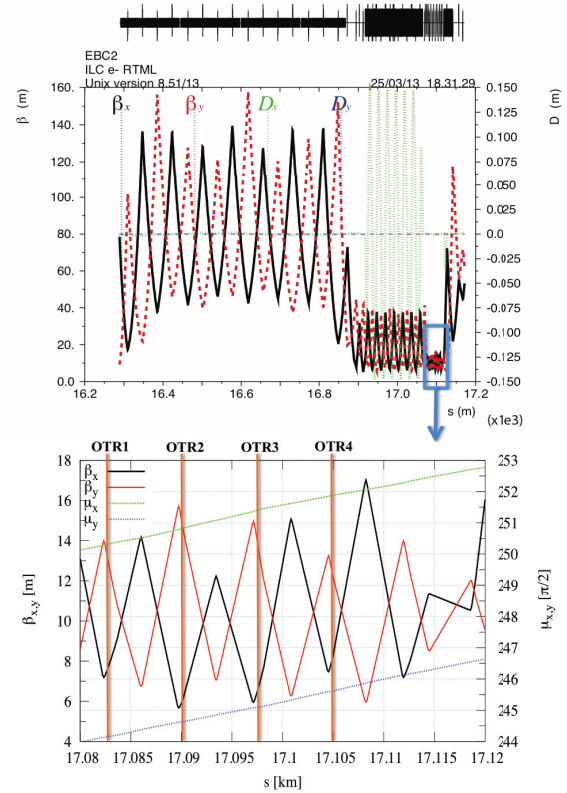


Figure 3: Optics layout of ILC BC2. Positions of 4 OTRs for a 2D emittance reconstruction section are indicated.

Table 2: Properties of materials.

Property	Kapton	Al	Be	Ti	W
$\sigma_{UTS}$ [MPa]	231	50	370	220	980
$Y$ [ $\times 10^5$ MPa]	0.025	0.68	2.87	1.16	4.11
$\alpha_T$ [ $\times 10^{-6}$ K $^{-1}$ ]	20	23.1	11.6	8.6	4.5
$k$ [W/(mK)]	0.12	210	200	17	163
$C_p$ [J/(gK)]	1.09	0.91	1.925	0.528	0.134
$\rho$ [g/cm $^3$ ]	1.42	2.7	1.85	4.54	19.3
$T_{melt}$ [K]	–	933.37	1546	1923	3643

Table 3. Since in this case the spot size is relatively big, for all the material studied the instantaneous temperature rise is below the fracture limit and far below the temperature excursion for melting ( $T_{melt} - 293 \text{ K}$ ). Therefore no damage is expected operating in single-bunch mode.

Table 3: Collision stopping power, instantaneous temperature rise and thermal fracture limit in the target material for OTR at the beginning of the ILC LTL.

Material	$\frac{dE}{dz}$ [MeV/cm]	$\Delta T_{inst}$ [K]	$\Delta T_{fr}$ [K]
Kapton	3.297	25.973	9240
Al	5.778	28.675	63.662
Be	3.704	12.682	222.28
Ti	9.112	46.35	441.06
W	32.366	152.6	1059.7

In the case of an OTR located in the diagnostic section at the end of the RTML (end of BC2):  $\sigma_x \approx 75.62 \mu\text{m}$

( $\beta_x \approx 7$  m) and  $\sigma_y \approx 5.34 \mu\text{m}$  ( $\beta_y \approx 14$  m). The corresponding results are shown in Table 4. In this case, stress fractures may be generated for targets made of Al, Ti and W. In principle, these calculations indicate that Kapton and Be might avoid damage. However, the use of Be could be discouraged due to costs and difficulties of machining (toxicity). Kapton could be a good candidate.

Table 4: Collision stopping power, instantaneous temperature rise and thermal fracture limit in the target material for OTR at the end of the ILC RTML.

Material	$\frac{dE}{dz} [\frac{\text{MeV}}{\text{cm}}]$	$\Delta T_{inst} [\text{K}]$	$\Delta T_{fr} [\text{K}]$
Kapton	3.665	298.81	9240
Al	5.996	307.96	63.662
Be	3.822	135.43	222.28
Ti	9.386	494.12	441.06
W	33.678	1643.3	1059.7

### M-OTR SYSTEM FOR THE CLIC RTML

A complete description of the CLIC RTML can be found in [6]. A preliminary design of the CLIC optics layout for 2D emittance reconstruction is shown in Fig. 4 [7], with  $\beta_x \approx 17.8$  m and  $\beta_y \approx 39.8$  m at the OTR positions. As in the previous section, for the study of the target damage analysis we will consider the case of a m-OTR system at the beginning of the RTML and other one at the RTML end. Table 5 summarises the corresponding beam parameters for these two cases.

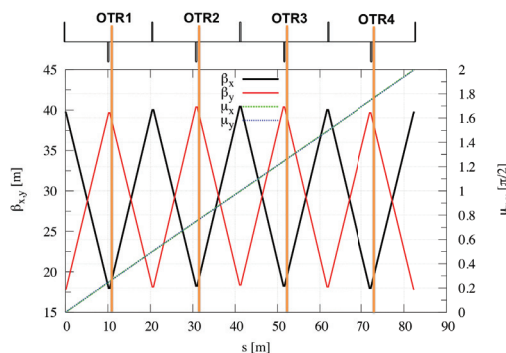


Figure 4: Optics layout of a 2D emittance measurement station for the CLIC RTML.

Table 5: Beam parameters at the beginning and at the end of the CLIC RTML.

Parameter	Start RTML	End RTML
Energy	2.86 GeV	9 GeV
Number of particles per bunch	$4 \times 10^9$	$3.72 \times 10^9$
Bunch length	1.8 mm	44 $\mu\text{m}$
Energy spread	0.12%	< 1.7%
Normalised H. emittance	500 nm	< 600 nm
Normalised V. emittance	5 nm	< 10 nm

### OTR Target Damage Study

Here we proceed as before and using Eq. (1) we calculate the temperature rise per pulse in single-bunch mode and compare it with the fracture limit, considering different material candidates for the OTR target in the context of an electron beam at the beginning (with  $\sigma_x \approx 39.88 \mu\text{m}$ ,  $\sigma_y \approx 5.96 \mu\text{m}$ ) and at the end (with  $\sigma_x \approx 24.62 \mu\text{m}$ ,  $\sigma_y \approx 4.75 \mu\text{m}$ ) of the RTML. The respective results are shown in Table 6 and Table 7. According to these results, in both cases Kapton, Be, Ti and W are below the fracture limit and Al surpasses such limit.

Table 6: Collision stopping power, instantaneous temperature rise and thermal fracture limit in the target material for OTR at the beginning of the CLIC RTML.

Material	$\frac{dE}{dz} [\frac{\text{MeV}}{\text{cm}}]$	$\Delta T_{inst} [\text{K}]$	$\Delta T_{fr} [\text{K}]$
Kapton	3.235	90.931	9240
Al	5.665	100.31	63.662
Be	3.633	44.383	222.28
Ti	8.935	162.17	441.06
W	31.691	533.12	1059.7

Table 7: Collision stopping power, instantaneous temperature rise and thermal fracture limit in the target material for OTR at the end of the CLIC RTML.

Material	$\frac{dE}{dz} [\frac{\text{MeV}}{\text{cm}}]$	$\Delta T_{inst} [\text{K}]$	$\Delta T_{fr} [\text{K}]$
Kapton	3.365	176.16	9240
Al	5.894	194.38	63.662
Be	3.779	85.984	222.28
Ti	9.302	314.44	441.06
W	33.061	1035.9	1059.7

### CONCLUSIONS

Multi-OTR systems can be used to make fast emittance measurements and contribute to the beam tuning in the RTML of linear colliders. They are intended to be used in single-bunch or low charge mode operation of the machine. This could be very useful during setup and commissioning phases. The key point is the selection of suitable materials to make OTR targets, which survive the impact of the pulses. According to the thermal calculations presented in this paper, Kapton and Be could be good candidates to be used as OTR radiators in the context of both the ILC and CLIC RTML.

### REFERENCES

- [1] A. Faus-Golfe et al., these Proceedings, MOPWO023.
- [2] S. T. Boogert et al., Phys. Rev. ST-AB **13**, 122801 (2010).
- [3] N. Solyak et al., Proc. of IPAC2012, TUPPR043.
- [4] A. Faus-Golfe and J. Navarro-Faus, "Emittance Reconstruction from Measured Beam Sizes", to be published.
- [5] <http://www.matweb.com>.
- [6] CLIC Conceptual Design Report, CERN-2012-007.
- [7] Y. A. Kubyshin et al., Proc. of IPAC2011, THP073.